

## Source Characteristics of Low Energy Storage Ring: MIRRORCLE-20

M. M. Haque<sup>1,2</sup>, A. Moon<sup>3</sup>, and N. Miura<sup>3</sup>

<sup>1</sup>Department of Photonics, Faculty of Science and Engineering, Ritsumeikan University, 1-1-1 Noji-higashi, Kusatsu, Shiga 525-8577, Japan

<sup>2</sup>Department of Physics, Faculty of Science, University of Rajshahi, Rajshahi-6205, Bangladesh

<sup>3</sup>Synchrotron Light Life Science Center, Ritsumeikan University, 1-1-1 Noji-higashi, Kusatsu, Shiga 525-8577, Japan

Received 10 June 2009, accepted in revised form 27 October 2009

### Abstract

The low energy storage ring MIRRORCLE-20, operating at electron energy  $E_{el} = 20$  MeV can produce a powerful infrared (IR) synchrotron radiation with wavelengths over mid-IR and far-IR regions. To clarify the applicability of this light source, its far-IR output as well as spectrum was measured. The IR emission is forced by a circular optics, named photon storage ring (PhSR), placed around the electron orbit, and is collected by a magic mirror associated with two plane mirrors in the storage ring. It is proven that the FIR intensity is boosted by the PhSR. The SR spectrum of MIRRORCLE-20 in the far-IR region is much broader and more intense than that of a typical black body light source, and therefore can be used for far infrared spectroscopy (FIRS).

*Keywords:* Storage ring; FIR source; 20 MeV MIRRORCLE; FIRS; FT/IR.

© 2010 JSR Publications. ISSN: 2070-0237 (Print); 2070-0245 (Online). All rights reserved.

DOI: 10.3329/jsr.v2i1.2637

J. Sci. Res. 2 (1), 9-16 (2010)

## 1. Introduction

Synchrotron radiation (SR) is useful for Terahertz (THz) or far infrared spectroscopy (FIRS) [1, 2]. Numerous beamlines that are dedicated to infrared spectroscopy have been developed at different SR facilities throughout the world. All of those are, however, extremely large machines, and are operated at very high electron energies,  $E_{el} = 700$ -8000 MeV. Third-generation synchrotron radiation sources certainly offer the necessary beam quality and brilliance, but they are too costly and are incompatible in industry, hospitals and research laboratories. Therefore, the number of users of these light sources is limited, and their usefulness for FIRS is not widely recognized. Because of these shortcoming of the third-generation synchrotrons, the necessity of laboratory sized light sources have been discussing since the last decade. Free-electron lasers (FEL) for far-IR source are rather quite compact. There are a number of such FEL centers in the world. FEL generates,

---

<sup>1</sup> Corresponding author: [mhpdr@gmail.com](mailto:mhpdr@gmail.com)

however, monochromatic far-IR, and it takes time for scanning over the wavelengths, which hinders using FEL for spectroscopy.

A far-IR laser by a tabletop synchrotron was proposed by Yamada in 1989 [3]. Such a tabletop synchrotron [4] has laid the foundation for the low energy storage rings MIRRORCLE, which are now the world smallest storage rings. Recently, a Compact Light Source (CLS) [5], operated at electron energy of 25 MeV, has been developed by Lyncean Technologies Inc. in USA for the purpose of X-ray imaging. A small ring has the advantages of: accumulating a large beam current from a small number of injected electrons, due to its small circumference, and suitability for forming relatively short bunches [6]. In addition, the small and exactly circular storage ring has a capacity to accommodate a circular mirror around the electron orbit. MIRRORCLE-type storage rings [7] are members of a series of low energy synchrotrons capable of generating a powerful infrared synchrotron radiation (IRSR) in the far infrared (FIR) region, as well as hard X-rays. MIRRORCLE radiates continuous spectrum covering from mid to far infrared. The spectrum is similar to those of large SR sources, and thus is useful for FIRS.

MIRRORCLE-20 [8, 9], operating at the electron energy of 20 MeV is a weak focusing type storage ring. The RF cavity operates at 2.45 GHz, the central orbit radius is of 156 mm, and the harmonic number is 8. Because of this small orbit radius the stored beam current easily reaches ampere order by one-shot injection within 100 ns injection time window and 100 mA injector beam current. The source characteristics of this small, low energy storage ring are of a significant practical interest.

In this paper are measured and analyzed the far-IR spectrum of MIRRORCLE-20. The enhancement of far-IR intensity, due to its special optical system, is also reported.

## 2. Beam Optics

Fig. 1(a) shows a schematic view of MIRRORCLE-20 FIR beamline. The optical system inside of MIRRORCLE-20 storage ring is somewhat different from usual SR beam optics. The special optical system is composed of an exactly circular concaved mirror (M0) concentric of the electron orbit, a magic mirror (M1) and two plane mirrors (M2 and M3).

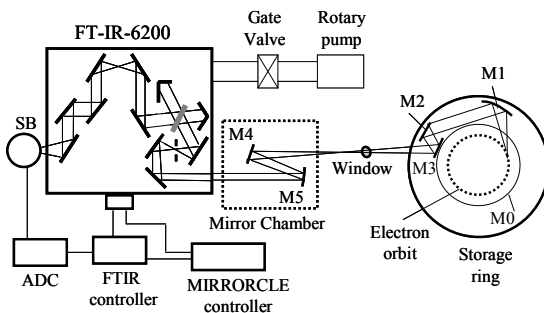


Fig. 1. (a) A schematic drawing of the far-IR beamline of MIRRORCLE 20. M0, M1 and M5 are the circular, magic and parabolic mirrors, respectively. M2, M3 and M4 all are plane mirrors. SB is silicon bolometer.

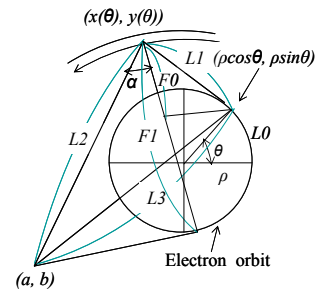


Fig. 1. (b) A schematic representation of the geometry of the magic mirror.  $\rho$  is the electron orbit radius,  $\theta$  the angle traveled by electron,  $\alpha$  the angle of reflection, respectively.

The circular mirror collects and accumulates synchrotron radiation (SR) photons emitted into  $2\pi$  of the electron orbit. Yamada has named this optical system as a “Photon Storage Ring (PhSR) [3]. The details about PhSR are described elsewhere [10]. The mirror M1, that is located at 290 mm from the center of the source, focuses SR photons from different position of electron beam trajectory, and mirrors M2 and M3 direct the radiation to the first focal point. The magic mirror of width 160 mm  $\times$  height 40 mm is capable of providing IR acceptance up to 355 (horizontal)  $\times$  138 (vertical) mrad<sup>2</sup>. However, the exit opening of mirror M0 for the present case limits the horizontal acceptance to 200 mrad. The horizontal acceptance of 355 mrad together with a bending radius of 156mm gives an emission length of 0.06 m.

Since the first focal point is located at 1.47 m from the focusing mirror (M1), it is difficult to get good focal conditions by using conventional spherical or elliptical mirrors. Therefore, we employed a three-dimensionally extended magic mirror proposed by Lopez- Delgado and Szwarc [11]. The magic mirror not only focuses the source but also reduces the time delay due to the large acceptance: the summation of the optical path length and the electron orbital length is the same for each emitting position [12]. Generally the shape of the magic mirror is described only by horizontal coordinates, but it also needs vertical curvature which depends on its position. From the schematic representation of the magic mirror (Fig. 1b), describing its horizontal and vertical geometry, it can be written;

$$L0 + L1 + L2 = cons. = d(say) \tag{1}$$

$$\frac{1}{R0} = \frac{1}{2} \left( \frac{1}{F0} + \frac{1}{F1} \right) \tag{2}$$

where,  $L0$  is the arc length traveled by an electron,  $L1$  the distance from the source point to the magic mirror,  $L2$  the distance from the magic mirror to its focal point,  $R0$  the vertical curvature of the magic mirror,  $F0$  &  $F1$  the projections of the source point and the focal point, respectively on the vertical axis of the magic mirror. Considering  $(x, y)$  to be the horizontal coordinates of the magic mirror,  $(a, b)$  its focal points coordinates,  $\theta$  the angle traveled by an electron,  $\alpha$  the angle of reflection,  $L3$  the distance from the focal point to the source point, and  $\rho$  the electron orbit radius, the following equations can be written;

$$L0 = \rho\theta \tag{3}$$

$$L1(\theta) = \{ [x(\theta) - \rho \cos \theta]^2 + [y(\theta) - \rho \sin \theta]^2 \}^{\frac{1}{2}} \tag{4}$$

$$L2(\theta) = \{ [x(\theta) - a]^2 + [y(\theta) - b]^2 \}^{\frac{1}{2}} \tag{5}$$

$$L3(\theta) = \{ (a - \rho \cos \theta)^2 + (b - \rho \sin \theta)^2 \}^{\frac{1}{2}} \tag{6}$$

$$F0(\theta) = L1(\theta) \cos[\alpha(\theta)] \tag{7}$$

$$F1(\theta) = L2(\theta) \cos[\alpha(\theta)] \tag{8}$$

$$y = -\frac{\cos\theta}{\sin\theta}x + \frac{\rho}{\sin\theta} \quad (9)$$

$$\alpha(\theta) = \frac{\cos^{-1}\left\{\frac{L1(\theta)^2 + L2(\theta)^2 - L3(\theta)^2}{2L1(\theta) \cdot L2(\theta)}\right\}}{2} \quad (10)$$

$$d = \rho\theta + \left\{[x(\theta) - \rho\cos\theta]^2 + [y(\theta) - \rho\sin\theta]^2\right\}^{\frac{1}{2}} + \left\{[x(\theta) - a]^2 + [y(\theta) - b]^2\right\}^{\frac{1}{2}} \quad (11)$$

$$\begin{aligned} R0(\theta) &= \frac{2F0(\theta) \cdot F1(\theta)}{F0(\theta) + F1(\theta)} \\ &= \frac{2L1(\theta) \cdot L2(\theta) \cdot \cos[\alpha(\theta)]}{L1(\theta) + L2(\theta)} \end{aligned} \quad (12)$$

Therefore, the horizontal and the vertical curvatures of the magic mirror can be calculated by solving the above equations. The parameters for MIRRORCLE-20 are  $\rho = 156$  mm,  $a = -750$  mm,  $b = -1400$  mm,  $d = 2200$  mm and  $\theta = 1.3\sim 1.5$  rad.

### 3. Experimental Conditions

The experiments were carried at MIRRORCLE-20, Synchrotron Light Life Science center, Ritsumeikan University. Beam injection was performed at 20 MeV by a circular microtron of 1.2 m outer diameter. A pulse klystron was used as a microwave source. The microtron injects electron pulse with a peak current  $I_p \leq 100$  mA, an injection time window  $T \leq 100$  ns, and an injection rate  $R_i \leq 100$  Hz. The number of electrons injected in one turn pulse is only  $6.7 \times 10^9$ , but the stored beam current is quite large compared with an ordinary synchrotron, because the orbit radius is small. These electrons circulate along 1 m long orbit, providing initially accumulated current of 3 A for the injector peak current of 100 mA. A magnetic field of 0.427 T is applied to the electron storage ring. The average beam current was monitored by a current transformer downstream of the bending magnet. The injection method provides 2/3-integer resonance, which is similar to the 1/2 resonance method used at AURORA [13]. It is known from simulation, as well as experiment, that the injection efficiency is nearly 100% [14, 15].

The IR beamline is equipped with a Fourier transform infrared spectrometer, FT-IR-6200 (JASCO Corp., Japan). It has a Michelson type interferometer, step scanning system for its moving mirror, and a function of time resolved measurements. A single point in an interferogram is measured by a single beam injection. The measurable wavelength is in the range between  $7800$   $\text{cm}^{-1}$  and  $20$   $\text{cm}^{-1}$ . The FT-IR main body can be exhausted by a rotary pump to avoid deposition of water vapor and carbon dioxide on the optical pass. The detector is a Si-bolometer (Infrared Lab, USA), unit 3118 of composite type, operating at a temperature of 4.2 K. The detector characteristics are: entrance aperture of 12.7 mm at a focal ratio of 3.8, exit aperture of 1.8 mm, area of 2.5 mm diameter diamond, and sensitivity of  $2.53 \times 10^5$  V/W.

## 4. Results and Discussion

### 4.1. Far-IR spectra

Far-IR spectrum from MIRRORCLE-20 was measured and compared with that from an internal blackbody light source of the FT-IR, while using the far-IR beamline shown in Fig. 1(a), and a step-scanning system. We employed a 25  $\mu\text{m}$  thick Mylar beamsplitter and a liquid He cooled Si bolometer. The detector included a cold low-pass filter to limit its bandwidth to wavenumbers below  $100\text{ cm}^{-1}$ . Other characteristics of the detector are mentioned in section 3. Spectra were collected with the spectrometer set to produce a resolution of  $0.25\text{ cm}^{-1}$ . The Jacquinot stop aperture of 2 mm diameter was used to achieve this resolution at  $100\text{ cm}^{-1}$ . The radiation window used in this measurement was a 3 mm thick TSURUPICA (Pakkusu, Japan). In comparison, a ceramic heater is a common blackbody light source used in the laboratory for the wavenumbers between  $100\text{ cm}^{-1}$  and  $10000\text{ cm}^{-1}$ . Off-line measurements of black body radiation from such a ceramic heater of size 7.1 mm $\Phi$  at 1300 K installed inside the spectrometer were performed in order to compare the SR spectrum with it. The optics including aperture, beam splitter and resolution were always the same for the measured spectra.

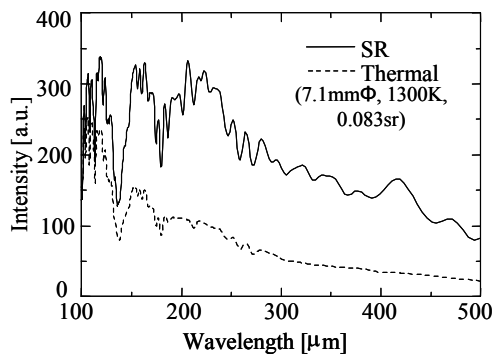


Fig. 2. Spectra measured from both MIRRORCLE-20 (solid line), and a thermal source (ceramic heater) at 1300 K (dotted line). Spectra were collected with the Michelson type FT/IR for the aperture size of 2 mm.

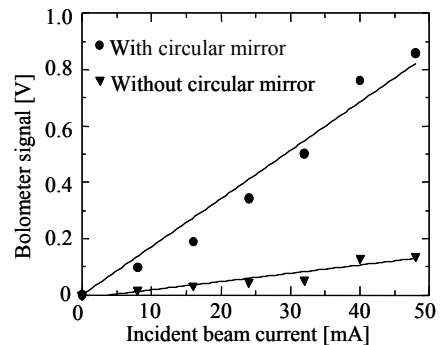


Fig. 3. Incident beam current dependency far-IR output measured by Si bolometer with and without PhSR. The injection rate was 15 Hz. At 48 mA beam current, the far-IR intensity is boosted about a factor of 7 by the PhSR.

Fig. 2 shows the spectra measured from both MIRRORCLE-20 and a standard blackbody light source. The solid line shows the SR spectrum, and the dotted line is for the thermal source. The spectra were taken at the injection beam current of 80 mA, which corresponds to the stored beam current of 1.2 A [16]. We note that the oscillatory structure of the spectral curve is partly caused by beam intensity variations from injection to injection. The drops near 138  $\mu\text{m}$  ( $72\text{ cm}^{-1}$ ) and 178  $\mu\text{m}$  ( $56\text{ cm}^{-1}$ ) are due to the absorption in the diamond wedged Crystal Quartz of bolometer filter and Mylar beamsplitter, respectively. The beamline does allow to be collected to lower wavenumber

of  $20\text{ cm}^{-1}$  (e.g.,  $500\text{ }\mu\text{m}$  using  $4.2\text{ K}$  bolometer), and more importantly, maintains the pulsed nature of the synchrotron source for use in broadband pump-probe spectroscopy [1]. The two sources provide a comparable signal at the detector, although the synchrotron outperforms the thermal source for the wavelengths longer than  $100\text{ }\mu\text{m}$ . For longer wavelength, the intensity of the thermal source decreases rapidly whereas that of synchrotron keeps at high level. At  $420\text{ }\mu\text{m}$  ( $\sim 23.5\text{ cm}^{-1}$ ) the synchrotron advantage approaches a factor of 5. In spite of a large thermal source at high temperature, the crossover point where the synchrotron outperforms the thermal source is substantially lower than that observed by other groups [17]. This is due to the advantages of the PhSR as well as the collection optics. The Michelson type interferometer's source is large (the source diameter is  $7.1\text{ mm}$  at  $1300\text{ K}$  in the present case), and the source collection optics serves the effective  $f$  number of  $f/3$ .

Unlike the laser nature, there is no monochromatic peak in the SR spectrum. Instead we observe a broad spectrum with enhanced radiation power over the far-IR/THz region. Such a broad spectrum has various applications in materials science and life science. Because, the terahertz dynamics is recently recognized to be important for these research fields. There is a technical border between optics and electronics, for this traditionally difficult spectra region. There is also a phenomenological overlapping area between diffusive motion of molecules and resonance of the chemical bonding as vibration. A new research field has already been opened for investigating the dynamics of proteins in water, and the related network structure of water using MIRRORCLE-20 far-IR beam [18].

The applications of far-IR with wavelengths between  $\sim 100\text{ cm}^{-1}$  and  $\sim 20\text{ cm}^{-1}$  are interesting, because time evolution involved in molecular and biological dynamics corresponds to this wavelength domain [19]. For example, the relaxation time of a molecular vibration is  $\sim 0.1\text{-}10\text{ ps}$ , the cycle of molecular vibration is  $\sim 10\text{-}100\text{ fs}$ , the revolution time of a molecule is  $\sim 1\text{ ps-}100\text{ ns}$ , the ionization time by light and proteins internal motion is  $>1\text{ ps}$ , and the relaxation time of formation by photosynthesis is  $3.5\text{ ps}$ . Furthermore, for DNA structures, Prohofsky and collaborators have predicted helix, base twisting, and librational modes in the  $20\text{-}100\text{ cm}^{-1}$  range [20-22]. Similarly, protein collective vibrational modes have been calculated to lie in the far infrared for bovine pancreatic trypsin inhibitor (BPTI) and human lysozyme [23, 24]. These all are in the wavelength domain observed in MIRRORCLE-20 far-IR spectrum.

### **4.3. Time resolved far-IR output**

The far-IR intensity was measured both with and without PhSR as a function of incident beam current. For this measurement a cooled Si-bolometer detector was placed directly at the surface position of the exit channel of the storage ring. Fig. 3 shows the measured intensity and their comparison. The solid lines indicate their corresponding linear fitting. The injection rate in this case was  $15\text{ Hz}$ . and the radiation window was a  $3\text{ mm}$  thick Tsurupica. At  $48\text{ mA}$  beam current, the far-IR intensity measured with PhSR is found to be about a factor of 7 higher than that measured without PhSR. The reader can see that this factor is very close to the length ratio of the circular mirror and mirror M1. This comparison indicates that the far-IR intensity is boosted by the PhSR.

A key characteristic of the PhSR is the reflection of collected SR photons to intersect the electron orbit again. This configuration, under certain circumstances, induces lasing and significantly boosts far-IR output by an order of magnitude. In this sense, the circular mirror surrounding the electron orbit also acts as an optical resonator, playing a great role

for high intense far-IR generation. The mirror fabricated for MIRRORCLE-20 is made of aluminum. This material is selected because of rigidity, and good IR reflectivity. Mirror curvature is made within 0.1  $\mu\text{m}$  tolerance. For 14  $\mu\text{m}$  wavelength and 156 mm electron orbit radius, we selected a mirror width,  $D = 20$  mm, a curvature in vertical direction,  $r_0 = 148$  mm, and a mirror radius,  $r = 216$  mm. The light pulses confined in the PhSR propagate along the single photon path finally leading to the exit opening, and form a pulse train with an exact time period. The Fourier transform of this pulse train corresponds to the frequency of the light wave.

## 5. Conclusions

In this article, we have presented the far-IR output as well as the spectrum of MIRRORCLE-20, which is equipped with an exactly circular optics (PhSR). The beamline is equipped with a Michelson's type FT-IR for covering the spectral range of 20-7800  $\text{cm}^{-1}$ . The present experiments demonstrate the potential of MIRRORCLE-20 for generating powerful far-IR radiation. We have proven the far-IR enhancement due to the PhSR mechanism. The SR spectrum of MIRRORCLE-20 maintains the pulsed nature, and in the far-IR region (longer than 100  $\mu\text{m}$ ) it is more intense than a typical black body light source. All these novel features will make MIRRORCLE-20 a useful light source for far infrared spectroscopy. We expect more intense far-IR by improving the IR collection efficiency and decreasing the electron beam size, in future.

## Acknowledgement

This work was supported by the 21<sup>st</sup> century COE program. The authors express sincere thanks to all members of the MIRRORCLE project and to the Master course students T. Kitagawa and Y. Nakamura for their help and discussion.

## References

1. R.P.S.M. Lobo, G.L. Carr, J. LaVeigne, D.H. Reitz and D.B. Tanner, *Rev. Sci. Instrum.* **73**, 1 (2002). [doi:10.1063/1.1416111](https://doi.org/10.1063/1.1416111)
2. P. Roy, J.-B. Brubach, P. Calvani, G. de Marzi, A. Filabozzi, A. Gerschel, P. Giura, S. Lupi, O. Marcouille, A. Mermet, A. Nucara, J. Orphal, A. Paolone, and M. Vervloet, *Nucl. Instrum. Methods Phys. Res. A* **467-468**, 426 (2001). [doi:10.1016/S0168-9002\(01\)00349-7](https://doi.org/10.1016/S0168-9002(01)00349-7)
3. H. Yamada, *Jpn. J. Appl. Phys.* **28** (9), L1655 (1989). [DOI: 10.1143/JJAP.28.L1665](https://doi.org/10.1143/JJAP.28.L1665)
4. H. Yamada, *Nucl. Instrum. Methods Phys. Res. B* **79**, 762 (1993). [doi:10.1016/0168-583X\(93\)95462-E](https://doi.org/10.1016/0168-583X(93)95462-E)
5. M. Bech, O. Bunk, C. David, R. Ruth, J. Rifkin, R. Loewen, R. Feidenhans and F. Pfeiffer, *J. Synchrotron Rad.* **16** (2009) 43. [doi:10.1107/S090904950803464X](https://doi.org/10.1107/S090904950803464X)
6. H. Yamada, *J. Synchrotron Rad.* **5**, 1326 (1998). [doi:10.1107/S0909049598007894](https://doi.org/10.1107/S0909049598007894)
7. H. Yamada, *AIP Conf. Proc.* **367**, 165 (1996).
8. H. Yamada, Y. Kitazawa, Y. Kanai, I. Tohyama, T. Ozaki, Y. Sakai, K. Sak, A.I. Kleev, G.D. Bogomolov, *Nucl. Instrum. Methods. A* **467-468**, (2001) 122. [doi:10.1016/S0168-9002\(01\)00238-8](https://doi.org/10.1016/S0168-9002(01)00238-8)
9. H. Yamada, *Nucl. Instrum. Methods Phys. Res. B* **199**, (2003) 509. [doi:10.1016/S0168-583X\(02\)01593-8](https://doi.org/10.1016/S0168-583X(02)01593-8)
10. Md. Monirul Haque, H. Yamada, A. Moon and M. Yamada, *J. Sci. Res.* **1** (1), 31 (2009). [doi: 10.3329/jsr.v1i1.1133](https://doi.org/10.3329/jsr.v1i1.1133)

11. R. Lopez-Delgado and H. Szwarc: *Opt. Commun.* **19**, 286 (1976).  
[doi:10.1016/0030-4018\(76\)90362-X](https://doi.org/10.1016/0030-4018(76)90362-X)
12. S. Kimura, H. Kimura, T. Takahashi, K. Fukui, Y. Kondo, Y. Yoshimatsu, T. Moriwaki, T. Nanba and T. Ishikawa, *Nucl. Instrum. Methods Phys. Res. A* **467-468**, 437 (2001).  
[doi:10.1016/S0168-9002\(01\)00351-5](https://doi.org/10.1016/S0168-9002(01)00351-5)
13. N. Takahashi, *Nucl. Instrum. Methods Phys. Res. B* **24/25**, 425 (1987).  
[doi:10.1016/0168-583X\(87\)90675-6](https://doi.org/10.1016/0168-583X(87)90675-6)
14. H. Yamada: *J. Vac. Sci. Technol. B* **8**, 1628 (1990). [doi.org/10.1116/1.585129](https://doi.org/10.1116/1.585129)
15. T Takayama, *Nucl. Instrum. Methods* **24/25**, 420 (1987). [doi:10.1016/0168-583X\(87\)90674-4](https://doi.org/10.1016/0168-583X(87)90674-4)
16. N. Miura A. Moon, H. Yamada, K. Nishikawa, T. Kitagawa, and N. Hiraiwa, Private communication (2009).
17. R.P.S.M. Lobo, J. LaVeigne, D.H. Reitze, D.B. Tanner, and G.L. Carr, *Rev. Sci. Instrum.* **70**, 2899 (1999). [doi:10.1063/1.1149846](https://doi.org/10.1063/1.1149846)
18. N. Miura, A. Moon, H. Yamada & T. Kitagawa, *AIP conf. Proc.* **902**, 73 (2007).  
[doi:10.1063/1.2723626](https://doi.org/10.1063/1.2723626)
19. G. R. Fleming and P. G. Wolynes, *Phys. Today*, 36 (1990). [doi:10.1063/1.881234](https://doi.org/10.1063/1.881234)
20. W. Zhuang, Y. Feng, & E. W. Prohofsky, *Phys. Rev. A* **41**, 7033 (1990).  
[doi:10.1103/PhysRevA.41.7033](https://doi.org/10.1103/PhysRevA.41.7033)
21. L. Young, V. V. Prabhu, E. W. Prohofsky and G. S. Edwards, *Phys. Rev. A* **41**, 7020 (1990).  
[doi:10.1103/PhysRevA.41.7020](https://doi.org/10.1103/PhysRevA.41.7020)
22. Y. Feng, W. Zhuang, & E. W. Prohofsky: *Phys. Rev. A* **43**, 1049 (1991).  
[doi:10.1103/PhysRevA.43.1049](https://doi.org/10.1103/PhysRevA.43.1049)
23. A. Roitberg, R. B. Gerder, R. Elber, & M. A. Ratner, *Science* **268**, 1319 (1995).  
[doi:10.1126/science.7539156](https://doi.org/10.1126/science.7539156)
24. S. Hayward & N. Go, *Annu. Rev. Phys. Chem.* **46**, 223 (1995).  
[doi:10.1146/annurev.pc.46.100195.001255](https://doi.org/10.1146/annurev.pc.46.100195.001255)